Journal of Fluids and Structures 120 (2023) 103907

Contents lists available at ScienceDirect

Journal of Fluids and Structures

journal homepage: www.elsevier.com/locate/jfs

Effects of inertia on the time-averaged propulsive performance of a pitching and heaving foil

R. Fernandez-Feria

Fluid Mechanics Group, Universidad de Málaga, Dr Ortiz Ramos s/n, 29071 Málaga, Spain

ARTICLE INFO

Article history:
Received 12 February 2023
Received in revised form 31 March 2023
Accepted 13 May 2023
Available online xxxx

Keywords:
Fluid–structure interaction
Propulsion
Swimming/flying

ABSTRACT

The inertia may play an important role in the unsteady behavior of a flapping foil. Of particular relevance in forward flapping locomotion is how the foil inertia may affect its time-averaged propulsive performance. This is the question addressed by the present study from a general, nonlinear formulation of the unsteady interaction with the surrounding fluid of a thin, flexible, two-dimensional and non-uniform foil undergoing prescribed pitching and heaving motion of any amplitude about an arbitrary pivot axis. For a rigid foil it is shown that, although the unsteady inertial forces and moments may be much larger than the unsteady aerodynamic forces and moments if the fluid density is much smaller than the foil density, the inertia does not affect the cycle-averaged propulsive performance for harmonic pitching and heaving motion, independently of their amplitude. Inertia may affect only the cycle-averaged moment if the mean angle of attack is not zero, but without affecting the cycle-averaged power input, and therefore the propulsive efficiency. When a small flexural deflection of the foil is considered, although the cycle-averaged inertial thrust and lift also vanish for any amplitude of the pitching and heaving harmonic motion, the cycle-averaged power input does not. Thus, the foil inertia contributes through the moment and power to the time-averaged propulsive performance for any flexural deflection of the foil, obtained her e analytically in terms of the trailing edge location for general pitching and heaving motion of any amplitude and phase and small flexural deflection amplitude. Simple analytical results are also provided for inertia dominated deflection, characterizing the conditions that minimize the power consumption. The results are valid for arbitrary chord-wise distribution of mass, thickness and (sufficiently large) stiffness of the foil.

© 2023 The Author(s). Published by Elsevier Ltd. This is an open access article under the CC BY-NC-ND license (http://creativecommons.org/licenses/by-nc-nd/4.0/).

1. Introduction

Inertia has been found to play a vital role in the structural dynamics of flapping foils, and therefore in their propulsive performance, obviously more markedly in aerial than in aquatic propulsion due to the much lower fluid/foil density ratio (Daniel and Combes, 2002; Combes and Daniel, 2003; Zhu, 2007; Michelin and Llewellyn Smith, 2009; Yin and Luo, 2010; Wu, 2011; Kang et al., 2011; Bergou et al., 2015; Olivier and Dumas, 2016; Shkarayev and Kumar, 2016; Zhang et al., 2017; Iverson et al., 2019). Although inertia is relevant for the instantaneous lift and thrust forces in aerial flapping flight even for rigid foils, it is for flexible foils where its effect becomes more important because the foil inertia contributes, together with the fluid forces, to the foil deformation, which in turn contributes to the unsteady aerodynamic forces and moments on the foil, thus doubly influencing the propulsive performance.

E-mail address: ramon.fernandez@uma.es.

https://doi.org/10.1016/j.jfluidstructs.2023.103907
0889-9746/© 2023 The Author(s). Published by Elsevier Ltd. This is an open access article under the CC BY-NC-ND license (http://creativecommons.org/licenses/by-nc-nd/4.0/).

Characterizing the contribution of inertia to the propulsive performance of a flapping foil is not an easy task because the complex, nonlinear fluid–structure problem which has to be solved numerically (Kang et al., 2011; Zhang et al., 2017; Goza and Colonius, 2017; Brousseau et al., 2021). This characterization is relevant even in experimental measurements, where the inertial forces and moments have to be subtracted from the measured reactions to obtain the aerodynamic force and moment, which is not an easy task for flexible foils (Yeo et al., 2013; Shkarayev and Kumar, 2016; Lankford and Chopra, 2022; Sanmiguel-Rojas et al., 2023). Fortunately, in some situations one may use simpler inviscid models, sometimes complemented with the small flapping amplitude assumption, from which the effect of inertia can be more easily computed, even analytically (Zhu, 2007; Alben, 2008; Michelin and Llewellyn Smith, 2009; Moore, 2014; Fernandez-Feria and Alaminos-Quesada, 2021).

In forward flapping locomotion one is mostly interested in the time-averaged propulsive performance, especially in the cycle-averaged thrust force and propulsive efficiency for periodic flapping kinematics. For a rigid foil, though it is known that the time-averaged power due to inertia vanishes for a purely heaving motion (Heathcote and Gursul, 2007; Kang et al., 2011), no general exact result for arbitrary flapping kinematics is available to the best of the author's knowledge, nor for the more general problem of a flexible foil. In the present work the inertial contributions to the flapping forces and moments are obtained from the general, nonlinear formulation of the unsteady interaction with the surrounding fluid of a thin, flexible, two-dimensional and non-uniform foil undergoing prescribed pitching and heaving motion of any amplitude about an arbitrary pivot axis. The theory is valid for arbitrary chord-wise distribution of mass, thickness and stiffness of the foil. Time averages of the inertial contributions to the thrust force and power input are obtained from these general expressions for harmonic kinematics assuming small flexural deflection amplitude, valid for sufficiently large stiffness of the foil.

2. Formulation of the problem

We consider a two-dimensional flexible foil of chord length c (when at rest) immersed in a uniform fluid stream of velocity U in the x direction and undergoing pitching and heaving motion about an arbitrary pivot axis located at $x = x_p$ and $z = h(t)$ in any instant of time t, where $h(t)$ is the heaving motion. The tangent to the foil centerline at this point has an angle with respect to the x axis $\alpha(t)$, corresponding to the pitching motion (see Fig. 1). The foil has variable density $\rho_s(s)$ and thickness $\varepsilon(s)$, where s is the Lagrangian coordinate along the foil centerline, $-s_i(t) \le s \le s_f(t)$, with $s = 0$ corresponding to the pivot axis, $s = -s_i(t)$ to the leading edge, and $s = s_f(t)$ to the trailing edge. The reference frame is such that, in absence of pitching and heaving motion, the foil centerline lies on the x axis between $-c/2$ and $c/2$, with the pivot axis at $x = x_p$. When pitch and/or heave are applied at the pivot axis, the foil moves according to the fluid–structure interactions but x_p remains fixed in the reference frame (x, z). The instantaneous chord length of the foil is $s_i(t) + s_f(t)$, approximately equal to c for large extensional rigidity (defined below).

For a thin beam ($\varepsilon/c \ll 1$) with structural bending rigidity EI, which in general depends on both s and t, and extensional rigidity characterized by a structural tension $T(s, t)$, the nonlinear equation of motion can be written as (Doyle, 2001)

$$\rho_s \varepsilon \frac{\partial^2 \mathbf{r}}{\partial t^2} - \frac{\partial}{\partial s}\left[T\frac{\partial \mathbf{r}}{\partial s}\right] + \frac{\partial^2}{\partial s^2}\left(EI\frac{\partial^2 \mathbf{r}}{\partial s^2}\right) = \mathbf{f}(s,t) + \mathbf{F}_p\delta(s) - \mathbf{g}\delta'(s)\,, \tag{1}$$

$$T(s,t) = E(s,t)\varepsilon(s)\left[1 - \left(\frac{\partial \mathbf{r}}{\partial s}\cdot\frac{\partial \mathbf{r}}{\partial s}\right)^{-1/2}\right], \qquad EI(s,t) = \frac{E(s,t)\varepsilon^3(s)}{12}\,, \tag{2}$$

where $\mathbf{r}(s, t)$ is the position vector of any point of the foil centerline s at the instant t. In the above equations

$$\mathbf{f} = \boldsymbol{\tau}^+\cdot\mathbf{n}^+ + \boldsymbol{\tau}^-\cdot\mathbf{n}^-\,, \qquad \boldsymbol{\tau} = -p\mathbf{I} + \mu\left(\nabla\mathbf{u} + (\nabla\mathbf{u})^T\right)\,, \tag{3}$$

is the Lagrangian force (per unit area) exerted on the plate by the surrounding fluid, where $\boldsymbol{\tau}$ is the fluid stress tensor, μ the fluid viscosity, $\mathbf{I}$ the unit tensor and $\mathbf{n}^+$ and $\mathbf{n}^-$ the unit normal vectors on each side of the plate at the given point $\mathbf{r}$ (see Fig. 1). The fluid pressure p and velocity $\mathbf{u}$ satisfy the Navier–Stokes equations with appropriate boundary conditions.

The last two terms in the right-hand side of Eq. (1) account for a point force $\mathbf{F}_p$ (per unit span) at the pivot axis, and for a point torque $\mathbf{M}_p$, modeled as a couple of opposite point forces $\pm\mathbf{g}$ at the pivot axis. Mathematically, the localized force is modeled by Dirac's delta function δ, and the localized torque by its derivative δ', as previously formulated by Fernandez-Feria and Alaminos-Quesada (2021) in the linearized limit and by Sanmiguel-Rojas et al. (2023) for the particular case of a purely pitching motion about the leading edge. Here arbitrary pitching and heaving motion about any pivot axis are considered to obtain general expressions for the inertial forces and moments.

$\mathbf{M}_p$ is the necessary torque to generate the pitching motion $\alpha(t)$, while the $z-$component of $\mathbf{F}_p$, F_{pz}, generates the heaving motion $h(t)$. The $x-$component of $\mathbf{F}_p$, F_{px}, fixes the location x_p of the pivot point on the x-axis of the reference frame (x, z) (see Fig. 1). This reference frame can be a stationary frame for a tethered foil immersed in a uniform current with velocity U along the $x-$direction at infinity, or a moving frame with the foil when it moves with velocity $-U\mathbf{e}_x$ in relation to a stationary fluid at infinity. In the first case, F_{px} is the reaction force needed to keep x_p fixed, and in the later case F_{px} is the total thrust force applied at the pivot axis to propel the foil with velocity $-U\mathbf{e}_x$. In either case, for given x_p, $h(t)$ and $\alpha(t)$, $\mathbf{F}_p$ and $\mathbf{M}_p$ must be such that they ensure the following constraint conditions at the pivot point $s = 0$:

$$\mathbf{r} = x_p\mathbf{e}_x + h(t)\mathbf{e}_z \equiv \mathbf{r}_p(t) \quad \text{and} \quad \frac{\partial \mathbf{r}}{\partial s} = \cos\alpha(t)\mathbf{e}_x + \sin\alpha(t)\mathbf{e}_z \equiv \mathbf{e}_\alpha(t) \quad \text{at} \quad s = 0\,, \tag{4}$$

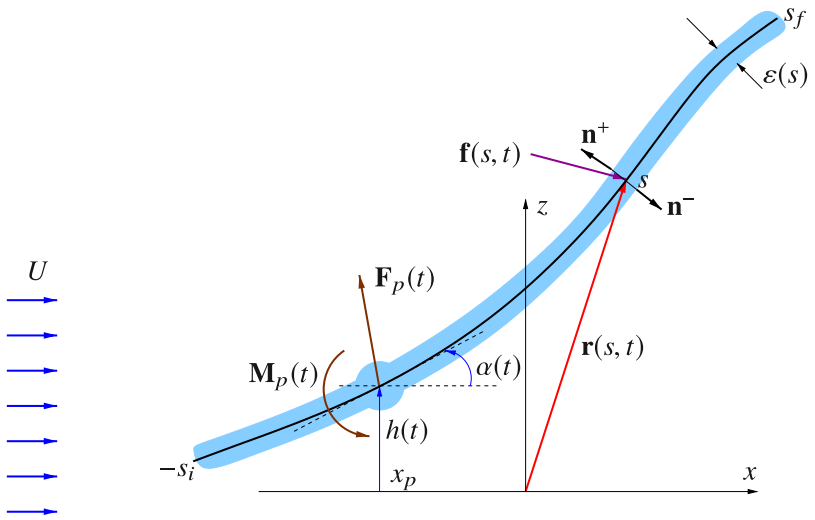

Fig. 1. Schematic of the flexible pitching and heaving foil (dimensional quantities).

where $\mathbf{e}_\alpha(t)$ is the unit vector tangent to the foil at the pivot point. On the other hand, the boundary conditions at the free leading and trailing edges of the foil are

$$-T\frac{\partial \mathbf{r}}{\partial s}+\frac{\partial}{\partial s}\left(EI\frac{\partial^2 \mathbf{r}}{\partial s^2}\right)=\mathbf{0}\,,\quad \frac{\partial^2 \mathbf{r}}{\partial s^2}=\mathbf{0}\quad \text{for}\quad s=-s_i\quad \text{and}\quad s=s_f\,. \tag{5}$$

If the pivot axis coincides with either the leading or the trailing edge, i.e., if $s_i=0$ or $s_f=0$, the corresponding boundary condition is modified to (4). The pivot axis location here is arbitrary, but inside the foil, excluding the exact locations of the leading or trailing edges.

2.1. Moment equations

Integrating Eq. (1) between $s=-s_i$ and $s=s_f$ and applying the above boundary conditions,

$$\int_{-s_i}^{s_f}\rho_s\varepsilon\,\frac{\partial^2 \mathbf{r}(s,t)}{\partial t^2}ds=\mathbf{F}(t)+\mathbf{F}_p(t)\,,\qquad \mathbf{F}(t)\equiv\int_{-s_i}^{s_f}\mathbf{f}(s,t)ds\,, \tag{6}$$

where $\mathbf{F}$ is the total force (per unit span) exerted by the fluid on the plate.

Likewise, multiplying Eq. (1) vectorially by $\mathbf{r}-\mathbf{r}_p$ and integrating, after using integration by parts and the boundary conditions, one gets

$$\int_{-s_i}^{s_f}\rho_s\varepsilon\,(\mathbf{r}-\mathbf{r}_p)\wedge\frac{\partial^2 \mathbf{r}(s,t)}{\partial t^2}ds=\mathbf{M}(t)+\mathbf{M}_p(t)\,, \tag{7}$$

where

$$\mathbf{M}(t)\equiv -M(t)\mathbf{e}_y=\int_{-s_i}^{s_f}(\mathbf{r}-\mathbf{r}_p)\wedge\mathbf{f}(s,t)ds\,,\quad \mathbf{M}_p(t)\equiv -M_p(t)\mathbf{e}_y=\mathbf{e}_\alpha(t)\wedge\mathbf{g}(t) \tag{8}$$

are the total bending moment (per unit span) with respect to the pivot axis that the fluid exerts on the airfoil and the external moment about the pivot axis, respectively. Both M and M_p are positive when counterclockwise.

Notice that Eqs. (6) and (7) are simpler than those obtained in Sanmiguel-Rojas et al. (2023), despite the fact that now a heaving motion is also included in the formulation, because the pivot point is not located at the leading edge. No structural terms associated to the extensional and bending rigidities enter into the moment Eqs. (6) and (7) if the external point force and the external moment are localized at an interior pivot point, however close to the foil ends.

For a flexible foil, we shall also use an additional *moment* of the beam Eq. (1). Multiplying it by s^2 and integrating between $s=-s_i$ and $s=s_f$, after using integration by parts twice and applying the boundary conditions, one obtains,

$$\int_{-s_i}^{s_f}\rho_s\varepsilon\,s^2\frac{\partial^2 \mathbf{r}(s,t)}{\partial t^2}ds+\int_{-s_i}^{s_f}2sT\frac{\partial \mathbf{r}(s,t)}{\partial s}ds+\int_{-s_i}^{s_f}2EI\,\frac{\partial^2 \mathbf{r}(s,t)}{\partial s^2}ds=\mathbf{D}(t)\,, \tag{9}$$

$$\mathbf{D}(t)\equiv\int_{-s_i}^{s_f}s^2\mathbf{f}(s,t)ds\,. \tag{10}$$

2.2. Nondimensional equations

To nondimensionalize the problem we use $c/2$, U and ρ as scaling factors, keeping the same symbols for the nondimensional variables, except for the fluid forces and moments, for which the usual coefficients are used:

$$C_L = \frac{F_z}{\frac{1}{2}\rho U^2 c}\,, \quad C_T = \frac{-F_x}{\frac{1}{2}\rho U^2 c}\,, \quad C_M = \frac{M}{\frac{1}{2}\rho U^2 c^2}\,, \quad C_{T_p} = \frac{F_{px}}{\frac{1}{2}\rho U^2 c}\,, \tag{11}$$

similarly C_{L_p} and C_{M_p}. Notice that the thrust coefficient C_T is positive when directed towards $-x$, as usual in propulsion aerodynamics, but we keep the same sign of C_{T_p} in relation to the $x-$component of $\mathbf{F}_p$. Thus, C_{T_p} is the nondimensional external force in the positive x direction that maintains the pivot point fixed at $x = x_p$, or, equivalently, it is the component in the direction $-x$ of the total propulsion force exerted by the fluid plus the inertia of the foil. Additionally, we define the *flexural* coefficients in the x and z directions as

$$C_{F_x} = \frac{D_x}{\rho U^2 (c/2)^3} \quad C_{F_z} = \frac{D_z}{\rho U^2 (c/2)^3}\,, \tag{12}$$

with D_x and D_z the components of $\mathbf{D}$ defined in Eq. (10).

However, to account for the chord-wise variation of the structural properties of the foil, they are not scaled with ρ, $c/2$ and U, but with their characteristic values (marked with subscript "0"), keeping also the same symbols for the nondimensional (order-of-unity) counterparts:

$$\rho_s(s) \leftarrow \rho_s(s)/\rho_{s_0}, \quad \varepsilon(s) \leftarrow \varepsilon(s)/\varepsilon_0, \quad E(s,t) \leftarrow E(s,t)/E_0, \quad T(s,t) \leftarrow T(s,t)/(E_0\varepsilon_0). \tag{13}$$

Thus, for a uniform plate with constant density, thickness and rigidity, the nondimensional functions $\rho_s(s) = \varepsilon(s) = E(s,t) = 1$ and $T(s,t) = [1 - |\partial\mathbf{r}/\partial s|^{-1}]$, with both $\mathbf{r}$ and s scaled with $c/2$.

Using these definitions, the nondimensional versions of Eqs. (6), (7) and (9) are

$$\frac{R}{2}\int_{-s_i}^{s_f} \rho_s\varepsilon\,\frac{\partial^2\mathbf{r}(s,t)}{\partial t^2}ds = (-C_T + C_{T_p})\mathbf{e}_x + (C_L + C_{L_p})\mathbf{e}_z\,, \tag{14}$$

$$\frac{R}{4}\int_{-s_i}^{s_f} \rho_s\varepsilon\,(\mathbf{r} - \mathbf{r}_p)\wedge\frac{\partial^2\mathbf{r}(s,t)}{\partial t^2}ds = -(C_M + C_{M_p})\mathbf{e}_y\,, \tag{15}$$

$$\frac{R}{2}\int_{-s_i}^{s_f} \rho_s\varepsilon\,s^2\,\frac{\partial^2\mathbf{r}(s,t)}{\partial t^2}ds + K\int_{-s_i}^{s_f} sT\,\frac{\partial\mathbf{r}(s,t)}{\partial s}ds + S\int_{-s_i}^{s_f} E\varepsilon^3\,\frac{\partial^2\mathbf{r}(s,t)}{\partial s^2}ds = C_{F_x}\mathbf{e}_x + C_{F_z}\mathbf{e}_z\,, \tag{16}$$

where

$$R = \frac{4\rho_{s_0}\varepsilon_0}{\rho c}\,, \quad K = \frac{4E_0\varepsilon_0}{\rho U^2 c}\,, \quad S = \frac{4E_0\varepsilon_0^3}{\rho U^2 c^3}\,, \tag{17}$$

are the mass ratio (or effective inertia), the nondimensional extensional rigidity and the nondimensional bending rigidity, respectively. Notice that for a uniform plate, $\int_{-s_i}^{s_f}\rho_s\varepsilon ds = s_f + s_i$.

If $K \to \infty$, Eq. (16) implies that $T \to 0$, so that the foil is inextensible ($|\partial\mathbf{r}/\partial s| = 1$ for any s and t) and $s_f + s_i = 2$. If, in addition, $S \to \infty$, that equation also implies that $\partial^2\mathbf{r}/\partial s^2 = 0$, and one has a rigid foil, where $\mathbf{r}(s,t)$ is a straight line (it is a linear function of s) for any t. This case will be considered first for simplicity.

3. Rigid foil

For a rigid foil, i.e., when K and S are both very large, the nondimensional position vector and its local acceleration can be written in terms of $h(t)$ and $\alpha(t)$ as

$$\mathbf{r}(s,t) = \mathbf{r}_p(t) + s\mathbf{e}_\alpha(t) = x_p\mathbf{e}_x + h(t)\mathbf{e}_z + s[\cos\alpha(t)\mathbf{e}_x + \sin\alpha(t)\mathbf{e}_z]\,, \tag{18}$$

$$\frac{\partial^2\mathbf{r}}{\partial t^2} = \ddot{h}\,\mathbf{e}_z + s\left[-\left(\dot{\alpha}^2\cos\alpha + \ddot{\alpha}\sin\alpha\right)\mathbf{e}_x + \left(-\dot{\alpha}^2\sin\alpha + \ddot{\alpha}\cos\alpha\right)\mathbf{e}_z\right]\,, \tag{19}$$

where dots denote derivatives with respect to nondimensional time t. Note that in this case $T = 0$ as $|\partial\mathbf{r}/\partial s| = |\mathbf{e}_\alpha| = 1$. Thus, in addition to the constraint (4) at the pivot point, Eq. (18) satisfies both boundary conditions (5), so that only Eqs. (14) and (15) are needed to relate the foil kinematics to the force and moment.

Substituting (19) into (14),

$$\frac{m}{2}R\left[\ddot{h} + s_0\left(\ddot{\alpha}\cos\alpha - \dot{\alpha}^2\sin\alpha\right)\right] = C_L + C_{L_p}\,, \tag{20}$$

$$-\frac{m}{2}Rs_0\left(\dot{\alpha}^2\cos\alpha + \ddot{\alpha}\sin\alpha\right) = -C_T + C_{T_p}\,, \tag{21}$$

where

$$m = \int_{-s_i}^{s_f} \rho_s \varepsilon ds\,, \quad ms_0 = \int_{-s_i}^{s_f} \rho_s \varepsilon s ds\,, \tag{22}$$

with s_0 the nondimensional position of the center of mass measured from the pivot axis at $s = 0$. Notice that $mRs_0/2$ is the nondimensional static moment. Remember that $m = 2$ for a uniform plate, with the center of mass at the center of the foil, $s_0 = (s_f - s_i)/2$. In classical aerodynamic notation (Theodorsen, 1935), $s_0 = -a$ in this case, or minus the location of the pivot point from the foil center.

Substituting (19) into (15), and taking into account that $\mathbf{e}_x \wedge \mathbf{e}_z = -\mathbf{e}_y$,

$$\frac{m}{4} R \left(s_0 \cos\alpha\, \ddot{h} + I_a\, \ddot{\alpha} \right) = C_M + C_{M_p}\,, \tag{23}$$

with

$$I_a = \frac{1}{m} \int_{-s_i}^{s_f} \rho_s \varepsilon s^2 ds = \frac{1}{6}(s_f^3 + s_i^3) = s_0^2 + \frac{1}{3}\,, \tag{24}$$

where I_a is the nondimensional moment of inertia, with the last two expressions in (24) corresponding to a uniform rigid plate [$s_0 = (s_f - s_i)/2$ and $s_f + s_i = 2$].

For given foil kinematics $h(t)$ and $\alpha(t)$, together with the expressions of the fluid force and moment, C_T, C_L and C_M, in terms of $h(t)$ and $\alpha(t)$, Eqs. (20) and (23) provide the total vertical force C_{L_p} and moment C_{M_p} on the pivot point needed to generate that kinematics, while (21) yields the total thrust force C_{T_p} that propels the foil. All these forces and moment are composed of a fluid component plus an inertial component,

$$C_{L_p} = -C_L + C_{L_R}\,, \quad C_{T_p} = C_T + C_{T_R}\,, \quad C_{M_p} = -C_M + C_{M_R}\,, \tag{25}$$

where the inertial parts C_{L_R}, C_{T_R}, and C_{M_R} are given by the right-hand sides of Eqs. (20), (21) and (23), respectively. Alternatively, if one measures experimentally the reactions C_{L_p}, C_{T_p} and C_{M_p} on the pivot axis together with the kinematics $h(t)$, $\alpha(t)$, Eqs. (20), (21) and (23) provide the fluid force and moment C_L, C_T and C_M. In either case, it is essential to dispose of explicit expressions for the inertial terms C_{L_R}, C_{T_R}, and C_{M_R} to evaluate the effect of inertia on the propulsive performance of a (rigid in the present case) flapping foil, which is the aim of the present work. In particular, we are mostly interested in the inertial contribution to the propulsion force

$$C_{T_R} = -\frac{m}{2} R s_0 \left(\dot{\alpha}^2 \cos\alpha + \ddot{\alpha} \sin\alpha \right)\,, \tag{26}$$

and in the inertial contribution to the power input needed to generate that thrust. The nondimensional power input at the pivot point can be written as

$$C_{P_p} = \dot{h} C_{L_p} + 2\dot{\alpha} C_{M_p} \equiv C_P + C_{P_R}\,, \quad \text{with} \quad C_P = -\dot{h} C_L - 2\dot{\alpha} C_M \tag{27}$$

the fluid contribution and

$$C_{P_R} = \dot{h} C_{L_R} + 2\dot{\alpha} C_{M_R} = \frac{m}{2} R \left\{ \dot{h} \left[\ddot{h} + s_0 \left(\ddot{\alpha} \cos\alpha - \dot{\alpha}^2 \sin\alpha \right) \right] + \dot{\alpha} \left(s_0 \cos\alpha\, \ddot{h} + I_a\, \ddot{\alpha} \right) \right\} \tag{28}$$

the inertial contribution. The quotient between C_{T_p} and C_{P_p} is related to the propulsive efficiency (see below), and therefore one has to evaluate the inertial contributions (26) and (28) to find out the effect of inertia of the propulsive efficiency of the foil.

Clearly, the inertial and fluid contributions to the propulsive performance are comparable to each other when R is of order unity, as it usually occurs in aerial flapping propulsion.

3.1. Harmonic pitch and heave

Consider the nondimensional heaving and pitching harmonic motion

$$h = h_0 \cos(kt)\,, \quad \alpha = \alpha_s + a_0 \cos(kt + \phi)\,, \quad k = \frac{\omega c}{2U}\,, \tag{29}$$

where h_0 and a_0 are the heave and pitch amplitudes, respectively, α_s a mean angle of attack, ϕ the pitch-heave phase lag and k the nondimensional (reduced) frequency associated to the physical flapping frequency ω. Substituting (29) into (26) and (28) one obtains the instantaneous inertial contribution to the propulsive performance, which is as relevant as the instantaneous contributions of the fluid forces and moment if R is not small.

But, in the cruising regime with this periodic flapping, one is more interested in cycle-averaged quantities. For any quantity $Z(t)$, its time average is defined as

$$\overline{Z} = \frac{k}{2\pi} \int_t^{t+2\pi/k} Z(t) dt\,. \tag{30}$$

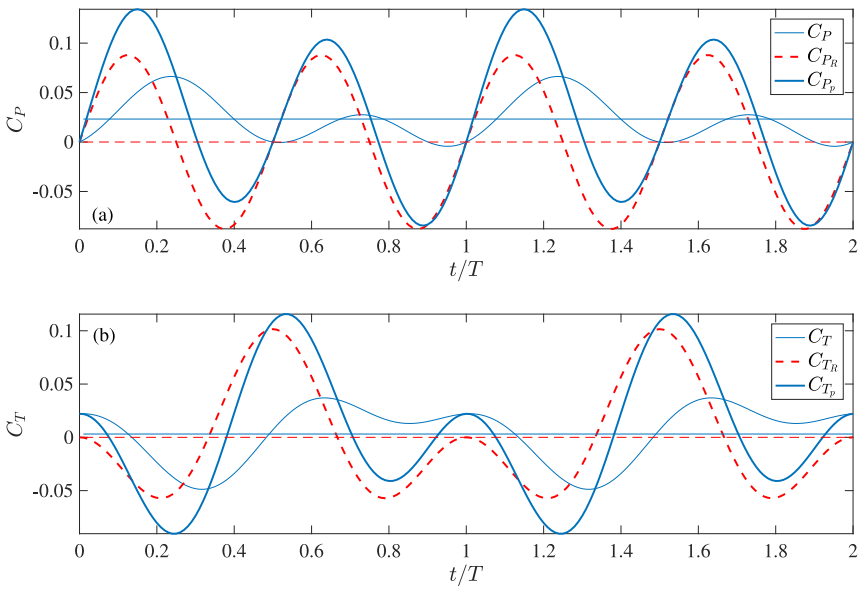

Fig. 2. Power (a) and thrust (b) coefficients vs. t/T ($T = 2\pi/k$) for $h_0 = 0.05$, $a_0 = 5°$, $\phi = 0$, $\alpha_s = -5°$, $s_0 = -a = 1/3$, $k = 1$, and $R = 20$. The horizontal lines are the corresponding time averages.

Interestingly, inserting (29) into Eqs. (26) and (28) and averaging, after some involved integrations of highly nonlinear expressions, it results that both $\overline{C}_{T_R}$ and $\overline{C}_{P_R}$ vanish (see Appendix A). This is so for *any amplitude and phase* of the flapping oscillations, even if the mean angle of attack is not zero, $\alpha_s \neq 0$. Therefore, the propulsive efficiency, defined as the ratio of $\overline{C}_{T_p}$ and $\overline{C}_{P_p}$, is independent of inertia for any value of R:

$$\eta = \frac{\overline{C}_{T_p}}{\overline{C}_{P_p}} = \frac{\overline{C}_T}{\overline{C}_P}\,. \tag{31}$$

This general result is very relevant because, despite the fact that instantaneous experimental measurements of the thrust force and power input may be quite affected by the inertial effects, especially in a wind tunnel, the cycle-averaged measurements are exactly the contributions coming from the fluid force and moment. Curiously, the time-averaged inertial moment does not vanish for a combined pitching and heaving motion with $\alpha_s \neq 0$ and a pivot axis that does not coincide with the center of mass, $s_0 \neq 0$ (see Appendix A):

$$\overline{C}_{M_R} = \pi \frac{m}{2} R s_0 k h_0 J_1(a_0) \cos(\phi) \sin(\alpha_s)\,, \tag{32}$$

where J_1 is the first order Bessel function of the first kind [for small amplitude, $a_0 \ll 1$, $J_1(a_0) \simeq a_0/2$]. However, when combined with C_{L_R} to obtain C_{P_R} according to (28), this cycle-averaged moment does not contribute to the time-averaged power input. Notice that these results are valid for any distribution of density and thickness of the foil, and therefore for any moment of inertia I_a.

To visualize how the instantaneous inertial thrust C_{T_R} and power C_{P_R} may be comparable to the fluid thrust and power, but only the fluid components contribute to their time averages, Fig. 2 shows, as an illustration, results for *small* pitch and heave amplitudes in a uniform rigid foil, for which the fluid contributions C_T and C_P are also obtained analytically (see Appendix B). A mass ratio $R = 20$ is used, corresponding to a typical aerial flapping propulsion with $\rho_s/\rho = 10^3$ and $\varepsilon/c = 5 \times 10^{-3}$. Further comparisons can be made using C_T and C_P computed numerically for higher pitch and heave amplitudes, and for any other set of the flapping parameters, since the analytical expressions for the inertial contributions C_{T_R} and C_{P_R} remain valid for any amplitude of the pitch and heave motions. But this is out of the scope of the present analysis, focused on the general analytical characterization of the inertial effects on the propulsive performance of a pitching and heaving foil.

4. Flexible foil

For a flexible foil we need at least an additional degree of freedom to characterize the foil motion, and, therefore, at least one more *moment* equation such as (9), or its nondimensional form (16), to characterize this new degree of freedom. A simple quadratic function of s like, for instance, $\mathbf{r}(s,t) = \mathbf{r}_p(t) + s\mathbf{e}_\alpha(t) + s^2\mathbf{d}(t)$, with new nondimensional vector $\mathbf{d}$ scaled with $2/c$, would be enough to account for the bending rigidity (EI) term in Eq. (9), and thus characterize the deflection

d in terms of the fluid forces through **D**. However, such a quadratic function, though satisfying the constraints (4) at the pivot point, cannot met the boundary conditions at the foil edges (5). To satisfy the boundary conditions at one of the foil edges (e.g., the trailing edge) one needs at least a quartic function of s. The simplest approximation is to assume that the pivot point is sufficiently close to the leading edge, so that for $-s_i \le s \le 0$ one may assume a rigid foil (which therefore satisfies automatically the boundary condition at the leading edge), and a quartic polynomial for $s \ge 0$:

$$\mathbf{r}(s,t) = \begin{cases} \mathbf{r}_p(t) + s\mathbf{e}_\alpha(t)\,, & -s_i \le s \le 0\,, \\ \mathbf{r}_p(t) + s\mathbf{e}_\alpha(t)(1 + t_1 s^2 + t_2 s^3) + s^2\mathbf{d}(t)(1 + d_1 s + d_2 s^2)\,, & 0 \le s \le s_f\,, \end{cases} \tag{33}$$

where t_1, t_2, d_1 and d_2 are nondimensional constants selected to satisfy the boundary conditions (5) at $s = s_f$; i.e.,

$$t_1 = -\left(\frac{T}{s^2 T + 2(\varepsilon_o/c)^2 E\varepsilon^3}\right)_{s=s_f}\,, \quad t_2 = \left(\frac{T}{2s^3 T + 4(\varepsilon_o/c)^2 sE\varepsilon^3}\right)_{s=s_f}\,, \tag{34}$$

$$d_1 = -\frac{4}{3}\left(\frac{sT + (\varepsilon_o/c)^2 E\varepsilon^3/s}{s^2 T + 2(\varepsilon_o/c)^2 E\varepsilon^3}\right)_{s=s_f}\,, \quad d_2 = -\frac{1}{6s_f^2} + \frac{4}{3}\left(\frac{sT + (\varepsilon_o/c)^2 E\varepsilon^3/s}{2s^3 T + 4(\varepsilon_o/c)^2 sE\varepsilon^3}\right)_{s=s_f}\,. \tag{35}$$

Although this is just an approximation for small deflection **d**, actually the simplest one satisfying all the boundary conditions, valid for sufficiently large bending stiffness S and pivot axis close to the leading edge, it allow us to obtain simple analytical expressions for the effect of flexibility on the inertial terms, and therefore to understand explicitly how flexibility may modify the above conclusions on the effect of inertia on the propulsive performance of a rigid foil. As shown in Fernandez-Feria and Alaminos-Quesada (2021), this approximation captures almost exactly the first natural frequency of the foil, but not the higher resonances. However, it is known that the best propulsive performance of a flexible flapping foil in terms of maximum time-averaged thrust and propulsive efficiency is reached at or near the first resonant mode of the foil for large enough bending stiffness, and for pivot axis close to the leading edge (Alben, 2008; Floryan and Rowley, 2018). The model can be simplified even further from the fact that, for a thin foil, $\varepsilon_0/c \ll 1$, the extensional stiffness is much larger than the bending stiffness, $K \gg S$, so that one may assume that $T \simeq 0$, and, consequently,

$$t_1 \simeq 0\,, \quad t_2 \simeq 0\,, \quad d_1 \simeq -\frac{2}{3s_f}\,, \quad d_2 \simeq \frac{1}{6s_f^2}\,. \tag{36}$$

Thus, Eq. (33) with (36) is the simplest approximation that takes into account the flexibility of a general nonuniform foil satisfying the boundary conditions (4)–(5), valid for large K and S, and a pivot point near the leading edge.

Defining the components of the nondimensional flexural deflection as

$$\mathbf{d}(t) = d_x(t)\mathbf{e}_x + d_z(t)\mathbf{e}_z\,, \tag{37}$$

substituting the above expressions into (14)–(16) and taking into account that

$$\mathbf{e}_\alpha \wedge \ddot{\mathbf{d}} + \mathbf{d} \wedge \ddot{\mathbf{e}}_\alpha = \mathbf{e}_y\left[-\ddot{d}_z\cos\alpha + \ddot{d}_x\sin\alpha - d_x(\ddot{\alpha}\cos\alpha - \dot{\alpha}^2\sin\alpha) - d_z(\ddot{\alpha}\sin\alpha + \dot{\alpha}^2\cos\alpha)\right], \tag{38}$$

$$\mathbf{d} \wedge \ddot{\mathbf{d}} = \mathbf{e}_y(-d_x\ddot{d}_z + d_z\ddot{d}_x)\,, \tag{39}$$

one obtains three equations similar to (20), (21) and (23) for a rigid foil, but with additional flexural deflection terms, plus two additional flexural equations for the components of **d**:

$$\frac{m}{2}R\left[\ddot{h} + s_0\left(\ddot{\alpha}\cos\alpha - \dot{\alpha}^2\sin\alpha\right) + g_2\ddot{d}_z\right] = C_L + C_{L_p}\,, \tag{40}$$

$$\frac{m}{2}R\left[-s_0\left(\dot{\alpha}^2\cos\alpha + \ddot{\alpha}\sin\alpha\right) + g_2\ddot{d}_x\right] = -C_T + C_{T_p}\,, \tag{41}$$

$$\begin{aligned}\frac{m}{4}R\Big\{ & s_0\cos\alpha\,\ddot{h} + I_a\ddot{\alpha} + g_2\ddot{h}d_x + h_d(d_x\ddot{d}_z - d_z\ddot{d}_x) \\ & + g_3\left[\ddot{d}_z\cos\alpha - \ddot{d}_x\sin\alpha + d_x(\ddot{\alpha}\cos\alpha - \dot{\alpha}^2\sin\alpha) + d_z(\ddot{\alpha}\sin\alpha + \dot{\alpha}^2\cos\alpha)\right]\Big\} = C_M + C_{M_p}\,,\end{aligned} \tag{42}$$

$$\frac{m}{2}R\left[I_a\ddot{h} + f_d\left(\ddot{\alpha}\cos\alpha - \dot{\alpha}^2\sin\alpha\right) + g_4\ddot{d}_z\right] + \mathcal{S}d_z = C_{F_z} \tag{43}$$

$$\frac{m}{2}R\left[-f_d\left(\dot{\alpha}^2\cos\alpha + \ddot{\alpha}\sin\alpha\right) + g_4\ddot{d}_x\right] + \mathcal{S}d_x = C_{F_x} \tag{44}$$

where the new nondimensional coefficients are

$$g_n = \frac{1}{m}\int_0^{s_f}\rho_s\varepsilon s^n\left[1 - \frac{2s}{3s_f} + \frac{1}{6}\left(\frac{s}{s_f}\right)^2\right]ds = \frac{26 + n(17 + 3n)}{12(n+1)(n+2)(n+3)}\,s_f^{n+1}\,, \quad n = 2, 3, 4, \tag{45}$$

$$h_d = \frac{1}{m}\int_0^{s_f} \rho_s \varepsilon s^4 \left[1 - \frac{2s}{3s_f} + \frac{1}{6}\left(\frac{s}{s_f}\right)^2\right]^2 ds = \frac{13}{405} s_f^5 \,, \tag{46}$$

$$f_d = \frac{1}{m}\int_{-s_i}^{s_f} \rho_s \varepsilon s^3 ds = \frac{1}{2}(s_f^4 - s_i^4) \,, \tag{47}$$

$$\mathcal{S} = \frac{2}{3} S \int_0^{s_f} E\varepsilon^3 \left(1 - \frac{s}{s_f}\right)^2 ds = \frac{2}{9} s_f \, S \,, \tag{48}$$

with the rightmost expressions of these coefficients corresponding to a uniform plate. From Eqs. (43) and (44) it is clear that the foil may be considered rigid (i.e., $d_x, d_z \to 0$) if the nondimensional bending stiffness $\mathcal{S} \to \infty$.

Given C_{F_x} and C_{F_z} as functions of $h(t)$, $\alpha(t)$, $d_x(t)$ and $d_z(t)$ and their temporal derivatives, and given the pitching and heaving motion, Eqs. (43)–(44) yield the flexural deflection components $d_x(t)$ and $d_z(t)$. Notice that to the flexural deflection contributes both the fluid force through C_F and the inertial force through the pitch and heave terms multiplied by R, being both contributions comparable in aerial propulsion. In fact, for some insect species it has been shown that wing deformation is mainly due to the wing inertia (Dudley, 2000; Combes and Daniel, 2003). Once $\mathbf{d}$ is known, together with the functions C_L, C_T and C_M in terms of $h(t)$, $\alpha(t)$ and $d_{x,z}(t)$, Eqs. (40) and (42) provide the reactions C_{L_p} and C_{M_p}, and consequently the power input

$$C_{P_p} = \dot{h} C_{L_p} + 2\dot{\alpha} C_{M_p} = C_P + C_{P_R} \,, \tag{49}$$

with

$$C_P = -\dot{h} C_L - 2\dot{\alpha} C_M \quad \text{and} \quad C_{P_R} = \dot{h} C_{L_R} + 2\dot{\alpha} C_{M_R} \,, \tag{50}$$

while Eq. (41) yields the thrust coefficient at the pivot point,

$$C_{T_p} = C_T + C_{T_R} \,. \tag{51}$$

In these expressions, C_{L_R}, C_{T_R} and C_{M_R} are the left-hand sides of Eqs. (40)–(42). The linearized limit of these equations, i.e., for small pitch and heave amplitudes, $|\alpha| \ll 1$, $|h| \ll 1$, and with small deflection only in the z direction, $d_x = 0$, $|d_z| \ll 1$, coincide with the equations derived in Fernandez-Feria and Alaminos-Quesada (2021) in the case of a uniform foil. In that work the problem was solved analytically for a harmonic motion with $\alpha_s = 0$. For the equivalence between the two sets of equations one has to take into account that in the linearized limit of the mentioned reference $x_p = a$, $s = x - a$, $s_0 = -a$, $s_i = 1 + a$, $s_f = 1 - a$, and that the sign of α has been changed. The present problem cannot be solved analytically owing to the nonlinear inertial terms in the left-hand sides of Eqs. (40)–(44) and, more importantly, because no general analytical expressions of the fluid coefficients in the right-hand sides of the equations are known analytically for large amplitudes of h, α and $\mathbf{d}$ [for small amplitudes these expressions were obtained in Alaminos-Quesada and Fernandez-Feria (2020)]. However, the time averages of the inertial terms in the left-hand sides of Eqs. (40)–(44) can be obtained analytically for a general harmonic motion, which is the main aim of the present work.

4.1. Inertial terms for a harmonic motion

For a harmonic pitching and heaving motion like (29), the flexural deflection (37) may eventually reach also a harmonic form, which in general can be written as

$$d_x = d_{xa}\cos(kt + \phi_x) \,, \quad d_z = d_{za}\cos(kt + \phi_z) \,. \tag{52}$$

Using these expressions and (29) one may compute the time averages of the inertial terms, resulting:

$$\overline{C}_{L_R} = 0 \,, \quad \overline{C}_{T_R} = 0 \,, \tag{53}$$

$$\overline{C}_{M_R} = \frac{R}{2} h_0 k^2 \left[S_0 J_1(a_0)\cos\phi \sin\alpha_s - \frac{g_2}{2} d_{xa}\cos\phi_1\right] \,, \tag{54}$$

$$\overline{C}_{P_R} = \overline{\dot{h} C_{L_R}} + 2\overline{\dot{\alpha} C_{M_R}} = -\frac{R}{2} k^3 \left[g_2 h_0 d_{za}\sin\phi_z + \right.$$
$$\left. 2g_3(J_1(a_0) - 2a_0 J_2(a_0))(d_{xa}\sin\alpha_s \sin(\phi - \phi_x) - d_{za}\cos\alpha_s \sin(\phi - \phi_z))\right] \,, \tag{55}$$

where J_1 and J_2 are the first and second order Bessel functions of the first kind, respectively. Therefore, for a flexible foil, the cycle-averaged inertial thrust remains zero for any small flexural deflection, independently of its origin, passive or forced, but the propulsive efficiency is affected by the inertia through a non-vanishing mean inertial power input. In the linearized limit, when $d_{xa} \simeq 0$ and $a_0 \ll 1$,

$$\overline{C}_{P_R} \simeq \frac{R}{2} k^3 d_{za} \left[-g_2 h_0 \sin\phi_z + g_3 a_0 \cos\alpha_s \sin(\phi - \phi_z)\right] \,. \tag{56}$$

So even without a mean angle of attack α_s there is a contribution of flexibility to the time-averaged power input from both heaving and pitching motions, provided that there is a phase shift of the flexural deflection in relation to any of them (remember that all the phase shifts are measured in relation to the heaving motion). This contribution may vanish or be negative for particular combinations of pitch and heave, thus enhancing the propulsive efficiency by minimizing the total power consumption. In the linear limit, when the power is given by (56), one may compute d_{za} and ϕ_z analytically for given pitching and heaving motion through Eq. (43) (Fernandez-Feria and Alaminos-Quesada, 2021). In general, the deflection amplitudes and phases, d_{xa}, d_{za}, ϕ_x and ϕ_z, can be obtained by just tracking the trailing edge position either numerically or experimentally. In the present nondimensional form the trailing edge location can be written as

$$\begin{aligned}\mathbf{r}(s=s_f,t) &= \left[x_p + s_f\cos[\alpha_s + a_0\cos(kt+\phi)]\right]\mathbf{e}_x + \left[h_0\cos(kt) + s_f\sin[\alpha_s + a_0\cos(kt+\phi)]\right]\mathbf{e}_z \\ &\quad + \frac{s_f^2}{2}\left[d_{xa}\cos(kt+\phi_x)\mathbf{e}_x + d_{za}\cos(kt+\phi_z)\mathbf{e}_z\right] \\ &\simeq \mathbf{e}_x + \{h_0\cos(kt) + (1-a)[\alpha_s + a_0\cos(kt+\phi)]\}\,\mathbf{e}_z + \frac{(1-a)^2}{2}d_{za}\cos(kt+\phi_z)\mathbf{e}_z\,, \end{aligned} \tag{57}$$

where the first two terms correspond to the motion as a rigid foil, and the last approximation is valid in the linear limit ($d_{xa} \simeq 0$, $h_0 \ll 1$, $a_0 \ll 1$, $x_p \simeq a$, $s_f \simeq 1-a$). Measuring the trailing edge location and knowing $h(t)$ and $\alpha(t)$, from this expression one may easily obtain d_{xa}, d_{za}, ϕ_x and ϕ_z, which inserted into (55) or (56) provides the cycle-averaged contribution of the inertia to the power input, independently of the origin of this flexural deflection.

4.2. Inertia dominated deflection

To gain more insight about the particular conditions for which deflection affects the time-averaged power, we consider here the simplest case when the flexural deflection is mainly determined by the inertia of the foil, as it often happens in aerial flapping locomotion (Dudley, 2000; Daniel and Combes, 2002). This situation occurs when the mass ratio R is sufficiently large and one may neglect the fluid contributions C_{F_x} and C_{F_z} to the deflection in Eqs. (43)–(44). To simplify further, we consider harmonic motion in the linear limit, so that only Eq. (43) is needed. Inserting (29) and (52) in complex form into (43), one obtains explicitly

$$d_{za}e^{i\phi_z} = \frac{k^2\left(I_a h_0 + f_d a_0 e^{i\phi}\right)}{g_4\left(\dfrac{2\mathcal{S}}{g_4\, mR} - k^2\right)}\,. \tag{58}$$

For any pitch an heave, the deflection amplitude peaks at the frequency

$$k = k_{r0} = \sqrt{\frac{2\mathcal{S}}{g_4\, mR}} = \sqrt{\frac{280}{71(1-a)^4}\frac{S}{R}}\,, \tag{59}$$

which corresponds to the first resonant frequency of the foil about the pivot axis in vacuum, the last expression for a uniform foil (in dimensional form, $\omega_{r0} \simeq (\varepsilon/c^2)\sqrt{E/\rho_s}$ for a pivot axis located at the leading edge, $a=-1$).

For a pure heaving or pitching motion, from Eq. (58) it results that $\phi_z = 0$ or $\phi_z = \phi$, respectively, so that the time-averaged power input vanish according to (56). Therefore, a combination of pitching and heaving motion with phase $\phi \neq 0$ is needed for the inertia to contribute to the time-averaged power input. Substituting (58) into (56) it turns out that $\overline{C}_{P_R} < 0$ for $k < k_{r0}$ and $\overline{C}_{P_R} > 0$ for $k > k_{r0}$ if $\phi < 180°$, and the opposite behavior is found if $\phi > 180°$. Thus, for a given pitch-heave motion with a phase shift smaller than 180° in a foil with structural properties and pivot point location characterized by a resonant frequency k_{r0}, to minimize the power consumption with the help of the inertial power one has to flap with a reduced frequency slightly smaller than k_{r0}. Conversely, if the reduced frequency k is fixed, one has to choose the structural properties and pivot point location of the foil such that k_{r0} is slightly larger than k. This general trend does not change much if the fluid contributions C_{F_x} and C_{F_z} to the flexural deflection is not negligible within the present approximation.

5. Conclusions

The following general results have been obtained for the cycle-averaged inertial effects on the propulsive performance of a foil undergoing harmonic pitching and heaving motion of any amplitude and phase about an arbitrary pivot axis and passive small flexural deflection. The cycle-averaged inertial contribution to the propulsive performance, if any, is of the order of the mass ratio R in relation to the fluid contribution.

- Inertial thrust and lift always vanish, $\overline{C}_{T_R} = \overline{C}_{L_R} = 0$, even for non-zero mean angle of attack ($\alpha_s \neq 0$), for any pitching any heaving motion and small flexural deflection.

- For a rigid foil, the time-averaged inertial moment does not vanish when a non-zero mean angle of attack is present, but it is negligible (it is quadratic in the heaving and pitching amplitudes) in the linear limit. In any case, this moment never contributes to the inertial cycle-averaged power input, $\overline{C}_{P_R} = 0$. Therefore, for a rigid foil, the inertia does not contribute to the cycle-averaged propulsive performance: both cycle-averaged thrust and propulsive efficiency come only from the fluid forces and moment, which simplifies the experimental measurement of these quantities with force/torque sensors.
- When some degree of flexibility is present in the foil, both the time-averaged moment and power input do not vanish even for null mean angle of attack, being both proportional to the flexural deflection amplitude. This flexural deflection can be computed from the analytical expressions given here by just following (either numerically or experimentally) the amplitude and phase of the trailing edge motion, thus allowing a straightforward computation of the inertial effects in the power input. In the linear limit the deflection can be obtained analytically.
- The cycle-averaged inertial power input does not vanishes when the flexural deflection is out of phase with the heaving and/or the pitching motions, and may become negative for certain kinematics, thus enhancing the propulsive efficiency by reducing the total power consumption. For inertially dominated deflection, reduction in the power consumption can be achieved only with combined, out of phase pitching and heaving motion, with a reduced frequency smaller (larger) than the first resonant frequency of the foil for phase shift smaller (larger) than 180°, the closer to the resonant frequency the larger the power reduction.

The analytical results given here for the inertial contributions to the propulsive performance of a two-dimensional flapping foil are valid for large extensional and bending rigidities and for a pivot axis location sufficiently close to the leading edge. These restrictions are in fact not very relevant because it is known that the best propulsive performance of a flexible flapping foil in terms of maximum time-averaged thrust and propulsive efficiency is reached at or near the first resonant mode of the foil for large enough bending stiffness, and for pivot axis close to the leading edge (Alben, 2008; Floryan and Rowley, 2018; Fernandez-Feria and Alaminos-Quesada, 2021). In fact, the quartic approximation used here for the small flexural deflection captures almost exactly the first natural frequency of the foil (Fernandez-Feria and Alaminos-Quesada, 2021). Obviously, the results are not directly applicable to a supper flexible foil, where higher resonances may play a relevant role. But the present analysis adds further insight, through analytical results, about the qualitatively different role played by the inertia on the propulsive performance of a foil undergoing small flexural deflections in relation to its rigid-foil counterpart. If the smallest flexural deflection modifies the inertial effects qualitatively, it is expected that larger and more complex flexural deflections would reinforce these differences quantitatively. The present results are valid for any chord-wise distribution of the foil density, thickness and stiffness (i.e., Young's modulus, provided that it is large enough) of the foil, and for any pitch and heave amplitude.

CRediT authorship contribution statement

R. Fernandez-Feria: Conceptualization, Methodology, Data curation, Formal analysis, Funding acquisition, Investigation, Project administration, Software, Supervision, Validation, Visualization, Writing – original draft, Writing – review & editing.

Declaration of competing interest

The authors declare that they have no known competing financial interests or personal relationships that could have appeared to influence the work reported in this paper.

Data availability

Data will be made available on request

Acknowledgments

This research has been supported by the Junta de Andalucía, Spain through grant UMA18-FEDER-JA-047.

Appendix A. $\overline{C}_{T_R}$, $\overline{C}_{P_R}$ and $\overline{C}_{M_R}$ for the harmonic motion of a rigid foil

The following integrals are performed with the help of the `Mathematica` software package. The integrals corresponding to the cycle averages of the two terms inside the parentheses in Eq. (26) for C_{T_R} are, when using the harmonic motion (29),

$$\int_0^{\frac{2\pi}{k}} [a_0 k \sin(kt+\phi)]^2 \cos[\alpha_s + a_0 \cos(kt+\phi)]\, dt = 2\pi k a_0 \cos(\alpha_s) J_1(a_0)\,, \tag{A.1}$$

$$\int_0^{\frac{2\pi}{k}} [-a_0 k^2 \cos(kt+\phi)] \sin[\alpha_s + a_0 \cos(kt+\phi)]\, dt = -2\pi k a_0 \cos(\alpha_s) J_1(a_0)\,, \tag{A.2}$$

where J_1 is the first order Bessel function of the first kind. Thus, the two terms cancel each other and $\overline{C}_{T_R} = 0$.

The integrals for the cycle averages of the five terms inside the curly brackets in Eq. (28) for C_{P_R} are

$$\int_0^{\frac{2\pi}{k}} h_0^2 k^3 \sin(kt)\cos(kt)\,dt = 0\,, \tag{A.3}$$

$$\int_0^{\frac{2\pi}{k}} a_0 h_0 k^3 s_0 \sin(kt)\cos(kt+\phi)\cos[\alpha_s + a_0\cos(f+kt)]\,dt = 2\pi h_0 k^2 s_0 [a_0 J_2(a_0) - J_1(a_0)]\cos(\alpha_s)\sin(\phi)\,, \tag{A.4}$$

$$\int_0^{\frac{2\pi}{k}} a_0^2 h_0 k^3 s_0 \sin(kt)\sin^2(kt+\phi)\sin[\alpha_s + a_0\cos(kt+\phi)]\,dt = -2\pi a_0 h_0 k^2 s_0 J_2(a_0)\cos(\alpha_s)\sin(\phi)\,, \tag{A.5}$$

$$\int_0^{\frac{2\pi}{k}} a_0 h_0 k^3 s_0 \cos(kt)\sin(kt+\phi)\cos[\alpha_s + a_0\cos(kt+\phi)]\,dt = 2\pi h_0 k^2 s_0 \cos(\alpha_s)\sin(\phi) J_1(a_0)\,, \tag{A.6}$$

$$\int_0^{\frac{2\pi}{k}} I_a a_0^2 k^3 \sin(kt+\phi)\cos(kt+\phi)\,dt = 0\,, \tag{A.7}$$

where J_2 is the second order Bessel function of the first kind. The three non-vanishing terms cancel each other, resulting $\overline{C}_{P_R} = 0$.

Finally, from Eq. (23), the inertial contribution to the moment is

$$C_{M_R} = \frac{m}{4} R\left(s_0\,\cos\alpha\,\ddot{h} + I_a\,\ddot{\alpha}\right)\,. \tag{A.8}$$

The time average of the second term vanishes for a harmonic motion, while that of the first term is given by Eq. (32).

Appendix B. C_P and C_T for a pitching and heaving rigid foil from linear potential flow theory

The following expressions for C_P and C_T are from Theodorsen (1935) and Fernandez-Feria (2016), respectively, but they are reproduced here because include the contributions from a mean angle of attack $\alpha_s \neq 0$, not considered in those works. In addition, they are written with both α and the moment positive when counterclockwise.

$$C_P = -\dot{h}\left\{\pi\left(-\dot{\alpha} - \ddot{h} + a\ddot{\alpha}\right) - 2\pi\alpha_s + \Re\left[\Gamma_0 \mathcal{C}(k)\right]\right\}$$

$$-\dot{\alpha}\left\{\frac{\pi}{2}\left[-\left(\frac{1}{2}-a\right)\dot{\alpha} + a\dot{h} - \left(a^2+\frac{1}{8}\right)\ddot{\alpha}\right] + \left(a+\frac{1}{2}\right)\pi\alpha_s - \frac{1}{2}\left(a+\frac{1}{2}\right)\Re\left[\Gamma_0\mathcal{C}(k)\right]\right\}, \tag{B.1}$$

$$C_T = \alpha C_L - \pi\dot{\alpha}\left(\dot{h} - a\dot{\alpha} + \alpha\right) + \left(\dot{h} - a\dot{\alpha} + \alpha\right)2\pi\alpha_s - \left(\dot{h} - a\dot{\alpha} + \alpha\right)\Re\left[\frac{2i}{\pi}\Gamma_0 \mathcal{C}_1(k)\right]$$
$$- \dot{\alpha}\Re\left[\Gamma_0\left(\frac{2}{\pi k}(1+ik)\mathcal{C}_1(k) + \frac{i}{k}\mathcal{C}(k)\right)\right], \tag{B.2}$$

with

$$C_L = \pi\left(-\dot{\alpha} - \ddot{h} + a\ddot{\alpha}\right) - 2\pi\alpha_s + \Re\left[\Gamma_0\mathcal{C}(k)\right] \tag{B.3}$$

being Theodorsen's lift coefficient (here positive upwards), Γ_0 given by

$$\Gamma_0 = -2\pi\left[\dot{h} + (\alpha - \alpha_s) - \left(a - \frac{1}{2}\right)\dot{\alpha}\right], \tag{B.4}$$

and the complex functions of the reduced frequency k

$$\mathcal{C}(k) = \frac{H_1^{(2)}(k)}{iH_0^{(2)}(k) + H_1^{(2)}(k)}\,, \quad \mathcal{C}_1(k) = \frac{\frac{1}{k}e^{-ik}}{iH_0^{(2)}(k) + H_1^{(2)}(k)}, \tag{B.5}$$

with $\mathcal{C}(k)$ the well known Theodorsen's function.

References

Alaminos-Quesada, J., Fernandez-Feria, R., 2020. Propulsion of a foil undergoing a flapping undulatory motion from the impulse theory in the linear potential limit. J. Fluids Mech. 883, 1–24, A19.

Alben, S., 2008. Optimal flexibility of a flapping appendage in an inviscid fluid. J. Fluids Mech. 614, 355–380.

Bergou, A.J., Swartz, S.M., Vejdani, H., Riskin, D.K., Reimnitz, L., Taubin, G., Breuer, K.S., 2015. Falling with style: Bats perform complex aerial rotations by adjusting wing inertia. PLoS Biol. 13 (11), 1002297.

Brousseau, P., Benaouicha, M., Guillou, S., 2021. Fluid–structure interaction effects on the deformable and pitching plate dynamics in a fluid flow. Appl. Ocean Res. 113, 102270.
Combes, S.A., Daniel, T.L., 2003. Into thin air: contributions of aerodynamic and inertial-elastic forces to wing bending in the hawkmoth Manduca sexta. J. Exp. Biol. 206 (17), 2999–3006.
Daniel, T.L., Combes, S.A., 2002. Flexible wings and fins: Bending by inertial or fluid-dynamic forces? Integr. Comput. Biol. 42, 1044–1049.
Doyle, J.F., 2001. Nonlinear Analysis of Thin-Walled Structures. Springer-Verlag, New York.
Dudley, R., 2000. The Biomechanics of Insect Flight. Princeton University Press, Princeton.
Fernandez-Feria, R., 2016. Linearized propulsion theory of flapping airfoils revisited. Phys. Rev. Fluids 1, 084502.
Fernandez-Feria, R., Alaminos-Quesada, J., 2021. Analytical results for the propulsion performance of a flexible foil with prescribed pitching and heaving motions and passive small deflection. J. Fluids Mech. 910, A43.
Floryan, D., Rowley, C.W., 2018. Clarifying the relationship between efficiency and resonance for flexible inertial swimmers. J. Fluids Mech. 853, 271–300.
Goza, A., Colonius, T., 2017. A strongly-coupled immersed-boundary formulation for thin elastic structures. J. Comput. Phys. 336, 401–411.
Heathcote, S., Gursul, I., 2007. Flexible flapping airfoil propulsion at low Reynolds numbers. AIAA J. 45, 1066–1079.
Iverson, D., Rahimpour, M., Lee, W., Kiwata, T., Oshkai, P., 2019. Effect of chordwise flexibility on propulsive performance of high inertia oscillating-foils. J. Fluids Struct. 91, 102750.
Kang, C.K., Aono, H., Cesnik, C.E.S., Shyy, W., 2011. Effects of flexibility on the aerodynamic performance of flapping wings. J. Fluids Mech. 689, 32–74.
Lankford, J.L., Chopra, I., 2022. Coupled aeroelastic study of a flexible micro air vehicle-scale flapping wing in hovering flight. J. Aircr. 59 (1), 154–172.
Michelin, S., Llewellyn Smith, S.G., 2009. An unsteady point vortex method for coupled fluid-solid problems. Theor. Comput. Fluids Dyn. 23, 127–153.
Moore, M.N.J., 2014. Analytical results on the role of flexibility in flapping propulsion. J. Fluids Mech. 757, 599–612.
Olivier, M., Dumas, G., 2016. Effects of mass and chordwise flexibility on 2D self-propelled flapping wings. J. Fluids Struct. 64, 46–66.
Sanmiguel-Rojas, E., Perona, J.L., Fernandez-Feria, R., 2023. Force and torque reactions on a pitching flexible airfoil. J. Fluids Mech. 961, A34.
Shkarayev, S., Kumar, R., 2016. Kinematics and inertial effects in locust flapping wings. Exp. Mech. 56, 245–258.
Theodorsen, T., 1935. General Theory of Aerodynamic Instability and the Mechanism of Flutter. Tech. Rep. TR 496, NACA.
Wu, T.Y., 2011. Fish swimming and bird/insect flight. Ann. Rev. Fluids Mech. 43, 25–58.
Yeo, D., Atkins, E.M., Bernal, L.P., Shyy, W., 2013. Experimental characterization of lift on a rigid flapping wing. J. Aircr. 50 (6), 1806–1821.
Yin, B., Luo, H., 2010. Effect of wing inertia on hovering performance of flexible flapping wings. Phys. Fluids 22, 111902.
Zhang, Y., Zhou, C., Luo, H., 2017. Effect of mass ratio on thrust production of an elastic panel pitching or heaving near resonance. J. Fluids Struct. 74, 385–400.
Zhu, Q., 2007. Numerical simulation of a flapping foil with chodwise or spanwise flexibility. AIAA J. 45, 2448–2457.